ELSEVIER

Applied Surface Science 186 (2002) 369–373

applied surface science

www.elsevier.com/locate/apsusc

Laser ablation of Ni by ultrashort pulses: molecular dynamics simulation

P.A. Atanasov[a,*], N.N. Nedialkov[a], S.E. Imamova[a], A. Ruf[b], H. Hügel[b], F. Dausinger[b], P. Berger[b]

[a]*Institute of Electronics, Bulgarian Academy of Sciences, 72 Tsarigradsko Shose, Sofia 1784, Bulgaria*
[b]*Institut für Strahlwerkzeuge, Universität Stuttgart, 43 Pfaffenwaldring, 70569 Stuttgart, Germany*

Abstract

Laser ablation of nickel has been investigated by the molecular dynamics simulation technique. The 500 fs laser pulses at $\lambda = 248$ nm were used in the simulations. The influence of the laser energy density on the process of ablation was studied. The time evolution of the plasma plume was shown. The threshold was determined and the ablation rate as a function of the laser energy density was obtained. The values are in good agreement with the experimental data of other authors. The dynamics of the shock wave in a solid was studied. The velocity of the ablated atoms and ions is several kilometers per second and increases with the laser fluence rise. © 2002 Elsevier Science B.V. All rights reserved.

Keywords: Laser ablation; fs Pulses; Molecular dynamics simulation; Nickel; Plasma plume; Shock wave

1. Introduction

Laser materials processing is being used widely in the industry for drilling, cutting, welding, scribing, etc. Among the various techniques, laser ablation finds a wide range of applications. This is why the laser ablation phenomenon is under intensive investigation. Its modeling requires the combination of several theoretical formulations from rather different areas of physics. Recently, the molecular dynamics (MD) simulations have demonstrated its potential for the detailed investigation of the mechanisms of laser ablation. These simulations allow one to obtain quantitative information, such as the energy, temperature, pressure, and velocity distributions that are often measured in the experiments, as well as qualitative pictures of atomic motions. Various materials, such as metals [1–3], semiconductors [4], or organic solids [5], have been explored by means of these techniques.

The ablation behavior and the dynamics of the removal process depend strongly on material's properties and parameters of the laser. That is why the choice of the ablation conditions is of crucial importance. Metals generally provide high absorption in the ultraviolet (UV) spectral range and the multi-photon absorption can be neglected in the sub-picosecond regime. Unlike in the cases of polymers and ceramics, the chemical effects can also be ignored. The experiments of some authors [6,7] on laser ablation of metals show some of the main advantages of using short pulses: during the pulse, no free plasma can develop and heat diffusion into the material is negligible. Consequently, the energy loss into the bulk is minimized and, as a result, the ablation threshold is reduced.

* Corresponding author. Tel.: +359-2-761423; fax: +359-2-975-3201.
E-mail address: paatanas@ie.bas.bg (P.A. Atanasov).

PII: S0169-4332(01)00683-3

Another important consequence is the minimal heat-affected zone which gives rise to the possibility of carrying out very precise and pure laser-processing of metals. The purpose of the following work is to study the ablation of nickel by 500 fs laser pulses at $\lambda = 248$ nm by the MD simulation technique. The influence of the laser energy density on the process of ablation was studied. The time evolution of the plasma plume was shown. The threshold was determined and the ablation rate as a function of the laser energy density was obtained and compared with the experimental data of other authors. The dynamics of the shock wave in a solid was studied.

2. Theory

Generally [8], the authors assume that the laser energy imparted into the material is transformed into heat. This induces phase transformation as melting, fusion, sublimation, or vaporization. It is known that electrons, atoms, and ions are produced in a high density plasma plume arising due to the laser irradiation. In order to clarify microscopically the ablation and vaporization phenomena, the material must be regarded not as a continuum but rather as an aggregate of atoms or molecules. It is difficult to observe the processing phenomena experimentally, because they occur in a very small region for a very short time interval. Consequently, the phenomena must be elucidated by theoretical analyses or simulation to the possible extent. The theoretical model elaborated here has the following main features:

- Laser wavelength is $\lambda = 248$ nm and pulse duration at $1/e$ level is $\tau_p = 500$ fs with a Gaussian temporal shape.
- Ni has a sufficiently high absorption coefficient ($\alpha = 1.25 \times 10^6\,\mathrm{cm}^{-1}$) and the reflection is $R = 0.475$ at this wavelength [7]. These parameters are assumed constant with the temperature.
- One-photon absorption is considered only when two- or multi-photon absorption can be neglected at energy densities lower than 10 J cm^{-2} [7].
- The laser-pulse energy is deposited into the material exponentially with the depth following the Lambert–Beer's law and results in a rise of the kinetic energy of the free electrons. The influence of the electron component is taken into account in the following manner, which is similar to that described in [9]. Every atom (free electron) accepts the energy of one photon during each act of interaction. The electrons thermalize in a few tens of femtoseconds. The atom is excited and if its energy exceeds the ionization energy (the first ionization potential for Ni is $U^{\mathrm{I}} = 7.63$ eV), it is transformed into an ion. This ionization energy is then taken away from the electron and it is not transferred to the lattice. The interaction between the Ni ions is governed by the Coulomb potential, which is added to the Morse one [10], used to describe the interaction between Ni atoms in the lattice. The energy stored by electrons is transferred to the lattice in the form of kinetic energy for a time interval $2\tau_{ei} \approx 1.1$ ps, where τ_{ei} is the electron–ion relaxation time, derived according to [11] as

$$\tau_{ei} \approx \left(\frac{M}{m_e}\right) v_{ei}^{-1}, \quad (1)$$

  where v_{ei} is the collision frequency between electrons and ions, M the atomic mass of Ni, and m_e the electron mass. This time interval is considered sufficient to ensure at least one order of magnitude decay of the electron energy.
- The simulation cell is restricted in x- and y-directions in order to increase the depth, while the latter is assumed to exceed 25 nm.
- The ablation takes place in vacuum.

Additionally, periodic boundary conditions are applied in the direction parallel to the surface. In this manner, the processes occurring in the center of the laser beam are being simulated. The velocity dampening technique is used on the bottom of the computational cell in order to minimize the effect of the shock wave reflection. Periodic boundary conditions in the x–y-directions are also applied above the material surface. Here, the simulation cell is not limited in the z-direction.

The time evolution of the system consisting of N particles is governed by Newton's second law. MD simulation is a technique which uses positions, velocities of the particles, and interaction potential as initial conditions to solve the equations of motion. As a result, the spatial ant temporal distribution of the energy, temperature, and pressure in the system, and the phase changes can be obtained. The velocity Verlet algorithm [12] is applied in order to integrate these equations.

The simulated system is configured in $4 \times 4 \times h\,(50 > h > 150)$ unit face-centered cubic cells. The starting conditions were taken as in the ideal crystal configuration at 0 K. An equilibrium in the simulation system was established at 300 K as a first step and then the laser pulse started.

3. Results and discussions

The evolution of the ablation process is presented in Fig. 1 for laser energy density of 0.1 J cm^{-2}. Here, 4.7×10^3 atoms are arranged in $4 \times 4 \times 70$ unit cells (the equivalent depth is 25 nm). The affected zone at 500 fs is about 2.5 nm and increases with the time; at 1 ps it exceeds 5 nm. The number of atoms ejected reaches its maximum at 3 ps. However, the ablated ions number reaches its maximum at about 1 ps. This is related to the Coulomb explosion, which also causes ejection of clusters. An interesting feature is the oscillation of the material's surface during the ablation, which is a result of the strong laser–matter interaction.

The temporal behavior of the plume is presented in Fig. 2. The first sharper maximum in the curve is composed dominantly by ions ablated by the Coulomb explosion. The second, much broader, maximum presents mainly the ablated Ni atoms. The ablation process is practically terminated at about 10 ps. Similar feature of the properties of ejected particles were obtained in [13] for the case of Si.

The velocity distribution of the atoms and ions ejected in the plasma plume is shown in Fig. 3. The values presented are evaluated when the particles reach the surface of the material at $z = 0$. The velocity distribution of the ions is non-Maxwellian, because of the non-thermal character of the ejection mechanism. The most probable velocity of ions (2.7 km s^{-1}) is higher than that (1.2 km s^{-1}) of the atoms, which is caused by the stronger Coulomb repulsive forces. It is worth pointed out that the particles (ions and atoms) will further be accelerated and will exchange the energy in the plume. The velocities of atoms and ions observed are of the same order of magnitude as the values obtained for other metals at slightly different

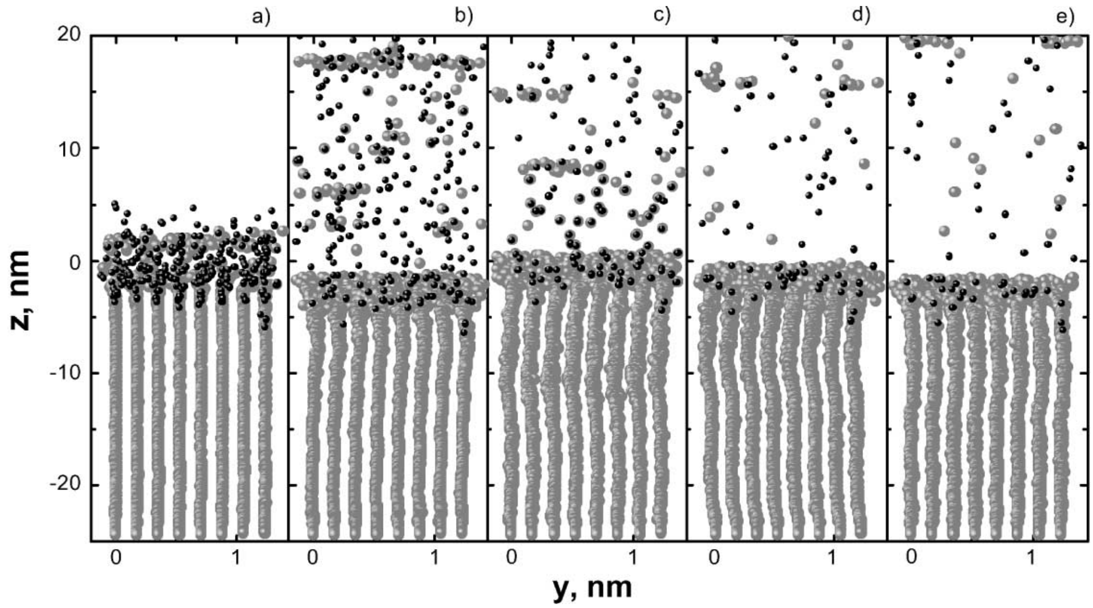

Fig. 1. Snapshots of the evolution of the ablation process in Ni: (a) 500 fs; (b) 1 ps; (c) 3 ps; (d) 6 ps; (e) 10 ps. The 4.7×10^3 atoms; $4 \times 4 \times 70$ unit cells; $E = 100$ mJ cm^{-2}; ions: black dots, atoms: gray.

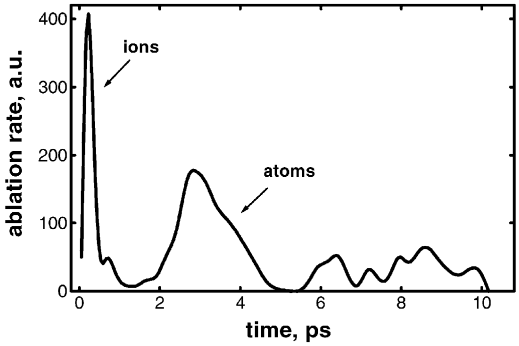

Fig. 2. Temporal behavior of the ablated particles: 6.4×10^3 atoms; $4\times4\times100$ unit cells; $E = 300\,\mathrm{mJ\,cm^{-2}}$.

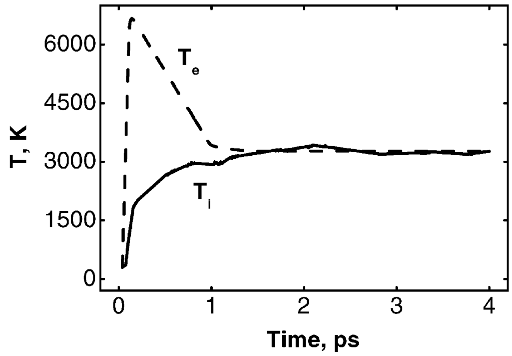

Fig. 4. Temporal dependence of the electron (dashed line) and lattice (solid line) temperatures, $E = 100\,\mathrm{mJ\,cm^{-2}}$.

experimental conditions [14,15]. The velocity distribution of metal atoms measured by time-of-flight mass spectroscopy is experimentally proven to be Maxwellian, see, for example [16,17]. Furthermore, the ion velocity distribution measured by time-of-flight technique is found to be near Maxwellian in Ti ablation by femtosecond laser pulses [18]. However, all these techniques measure the particle velocities at sufficient distances far from the material surface. Moreover, our values and velocity distributions (Fig. 3) are valid for the Ni surface, as it was mentioned above. Additionally, we believe that the presence of electrons in the consideration will not dramatically influence on the ion velocity distribution.

The temporal dependence of the electron and lattice temperatures of the system at $E = 100\,\mathrm{mJ\,cm^{-2}}$ is presented in Fig. 4. The electron temperature is estimated according to the two-temperature model [6] using the following values of the physical parameters:

- $A = 1 - R = 0.525$; $\alpha = 1.25\times10^8\,\mathrm{m^{-1}}$.
- Density of the free electrons in Ni, $n_e = 7.3\times10^{29}\,\mathrm{m^{-3}}$; $U^I = 7.63\,\mathrm{eV}$; $\tau_{ei} = 0.55\,\mathrm{ps}$.
- Laser power density, $I_0 = 2\times10^{15}\,\mathrm{W\,m^{-2}}$; $\tau_p = 0.5\,\mathrm{ps}$ ($1/e$ level).
- Specific heat constant, $a_e = 1065\,\mathrm{J\,m^{-3}\,K^{-2}}$; thermal conductivity, $K_e = 91\,\mathrm{W\,m^{-1}\,K^{-1}}$ (at 300 K); lattice heat capacity, $C_i = 4.1\times10^6\,\mathrm{J\,m^{-3}\,K^{-1}}$. The values of a_e, K_e and C_i were taken from Wellershoff et al. [19].

The evaluation of the forces acting on every atom in the system gives information on the formation and propagation of the shock wave. The propagation of the shock wave in-depth of the material is shown in Fig. 5.

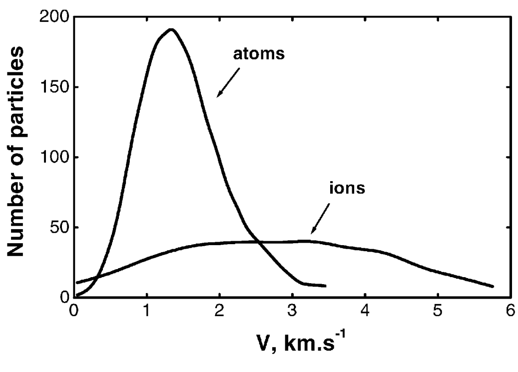

Fig. 3. Velocity distribution of the ablated atoms and ions in the plasma plume: 6.4×10^3 atoms; $4\times4\times100$ unit cells; $E = 200\,\mathrm{mJ\,cm^{-2}}$.

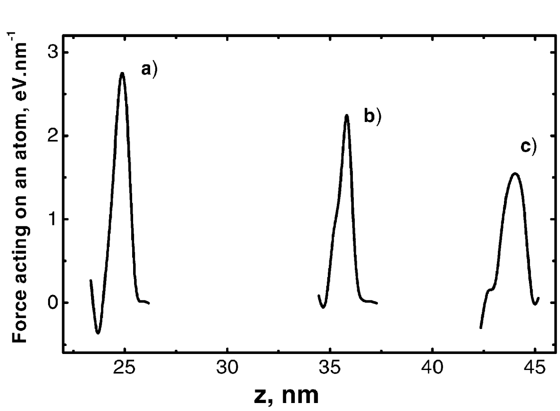

Fig. 5. The shock wave evolution in Ni, $E = 100\,\mathrm{mJ\,cm^{-2}}$: (a) 1 ps; (b) 1.5 ps; (c) 2 ps.

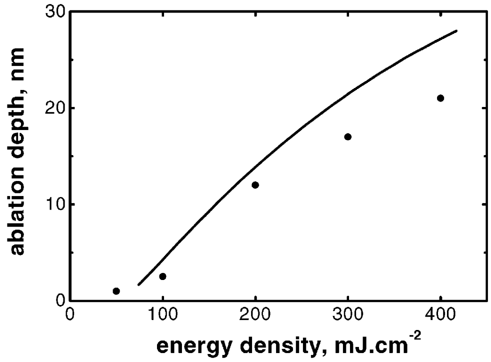

Fig. 6. Dependence of the ablation depth on the energy density: solid line represents MD simulation results; circles represents experimental data [7].

The velocity values evaluated are 22.1 and 16.5 km s^{-1} for the time intervals 1.0–1.5 and 1.5–2.0 ps, respectively; the shock wave velocity and its amplitude decrease with the time. For comparison, the sound velocity in Ni is 4.97 km s^{-1}. However, the sound is only very small disturbance compare to shock wave. It will reach this value deeper in the material. Such high value of the shock wave is related mainly to the ions expulsion since the time intervals for shock wave evolution are taken close to the beginning of the ablation process. The shock wave propagation inside the solid disturbs the lattice in-depth as is seen from Fig. 1.

The relationship between ablation depth and energy fluence is presented in Fig. 6. There are no ablated atoms at fluences lower than 70 mJ cm^{-2}, which may be considered as the ablation threshold. It is seen that there is a good coincidence between the theoretical curve and the experimental data taken from Preus et al. [7]. However, the discrepancy between the theoretical values and the experimental ones is increased with the laser density rise and reaches about 20% at $E = 400\,\mathrm{mJ\,cm^{-2}}$. This may be related to the constant values of Ni optical parameters taken in the model.

4. Conclusion

The MD method was applied to the description of the process of laser ablation of Ni by 500 fs UV laser pulses. The main results obtained are:

- Temporal behavior of the ablated particles (ions and atoms) is obtained and their velocity distribution in the plume is determined. The velocities of the ablated atoms are several kilometers per second, which are lower than those of the ions, and increase when the laser fluence rises.
- The velocity of the shock wave propagating very close to the solid surface is determined to be 16.5 km s^{-1} and it decreases inside the material. Then, it will reach the sound velocity in Ni.
- The ablation threshold is determined to be about 70 mJ cm^{-2}. The value is in good agreement with the experimental data.

Acknowledgements

This work is supported financially in part by the BMBF project N:13N7710/6 (PRIMUS), Germany.

References

[1] E. Ohmura, I. Fukumoto, Int. J. Jpn. Soc. Prec. Eng. 30 (1996) 128.
[2] E. Ohmura, I. Fukumoto, Int. J. Jpn. Soc. Prec. Eng. 30 (1996) 47.
[3] E. Ohmura, I. Fukumoto, I. Miyamoto, Proc. ICALEO, Ser. A (1998) 45.
[4] R.F.W. Herrmann, J. Gerlach, E.E.B. Campbell, Nucl. Instrum. Meth. Phys. Res. B 122 (1997) 401.
[5] L.V. Zhigilei, P.B.S. Kodali, B.J. Garrison, J. Phys. Chem. B 102 (1998) 2845.
[6] B.N. Chichkov, C. Momma, S. Nolte, F. von Alvensleben, A. Tünnermann, Appl. Phys. A 63 (1996) 109.
[7] S. Preus, A. Demchuk, M. Stuke, Appl. Phys. A 61 (1995) 33.
[8] D. Bäuerle, Laser Processing and Chemistry, 3rd Edition, Springer, Berlin, 2000, pp. 221–257.
[9] R.F.W. Herrmann, J. Gerlach, E.E.B. Campbell, Appl. Phys. A 66 (1998) 35.
[10] I.A. Girifalco, V.C. Weizer, Phys. Rev. 114 (1959) 687.
[11] W.L. Kruer, The Physics of Laser Plasma Interaction, Addison-Wesley, New York, 1987.
[12] M.P. Allen, D.J. Tildesley, Computer Simulation of Liquids, Clarendon Press, Oxford, 1987.
[13] R.F.W. Herrmann, J. Gerlach, E.E.B. Campbell, Nucl. Instrum. Meth. Phys. Res. B 122 (1997) 401.
[14] H. Wang, A.P. Salzberg, B.R. Weiner, Appl. Phys. Lett. 59 (1991) 935.
[15] R. Stoian, D. Ashkenasi, A. Rosenfeld, M. Wittmann, R. Kelly, E.E.B. Campbell, Nucl. Instrum. Meth. Phys. Res. B 166–167 (2000) 682.
[16] I. Zergioti, M. Stuke, Appl. Phys. A 67 (1998) 391.
[17] J.C.S. Kools, J. Dieleman, J. Appl. Phys. 74 (1993) 4163.
[18] M. Ye, C.P. Grigoropoulos, J. Appl. Phys. 89 (2001) 5183.
[19] S.-S. Wellershoff, J. Hohlfeld, J. Güdde, E. Matthias, Appl. Phys. A 69 (1999) S99.